Original Article

VLA-4 mediated adhesion of melanoma cells on the blood–brain barrier is the critical cue for melanoma cell intercalation and barrier disruption

Ana B García-Martín[1], Pascale Zwicky[1], Thomas Gruber[1] (iD),
Christoph Matti[1], Federica Moalli[1], Jens V Stein[1],
David Francisco[2], Gaby Enzmann[1], Mitchell P Levesque[3],
Ekkehard Hewer[4] (iD) and Ruth Lyck[1] (iD)

Abstract

Melanoma is the most aggressive skin cancer in humans. One severe complication is the formation of brain metastasis, which requires extravasation of melanoma cells across the tight blood–brain barrier (BBB). Previously, VLA-4 has been assigned a role for the adhesive interaction of melanoma cells with non-BBB endothelial cells. However, the role of melanoma VLA-4 for breaching the BBB remained unknown. In this study, we used a mouse in vitro BBB model and imaged the shear resistant arrest of melanoma cells on the BBB. Similar to effector T cells, inflammatory conditions of the BBB increased the arrest of melanoma cells followed by a unique post-arrest behavior lacking immediate crawling. However, over time, melanoma cells intercalated into the BBB and compromised its barrier properties. Most importantly, antibody ablation of VLA-4 abrogated melanoma shear resistant arrest on and intercalation into the BBB and protected the BBB from barrier breakdown. A tissue microarray established from human brain metastasis revealed that indeed a majority of 92% of all human melanoma brain metastases stained VLA-4 positive. We propose VLA-4 as a target for the inhibition of brain metastasis formation in the context of personalized medicine identifying metastasizing VLA-4 positive melanoma.

Introduction

Melanoma is a malignant tumor that originates from melanocytes, which are the normal pigment producing cells in the skin and the uvea of the eye. Brain metastasis of melanoma is a severe complication that dramatically lowers the overall survival.[1,2] However, treatment strategies to prevent metastasis formation are still rare.[3] A better understanding of the formation of melanoma metastasis is an urgent medical need in order to develop personalized treatment strategies.

In general, cancer metastasis formation is a multi-step process that is initiated through invasion, followed by intravasation into blood or lymphatic vessels, survival in the circulation, arrest at distant sites, extravasation out of the circulation, and finally micro- and macro-metastasis establishment.[4] For the development of brain metastases, melanoma cells have to breach the blood–brain barrier (BBB). The BBB is

[1]Theodor Kocher Institute, University of Bern, Bern, Switzerland
[2]Interfaculty Bioinformatics Unit, University of Bern, Bern, Switzerland
[3]Department of Dermatology, University of Zurich Hospital, University of Zurich, Zurich, Switzerland
[4]Institute of Pathology, University of Bern, Bern, Switzerland

Corresponding author:
Ruth Lyck, Theodor Kocher Institute, University of Bern, Freiestrasse 1, P.O Box 938, Bern 9 CH-3000, Switzerland.
Email: ruth.lyck@tki.unibe.ch

formed by microvascular endothelial cells (ECs) that are tightly sealed by specialized tight junctions.[5] Thus, the BBB establishes a particularly tight endothelial barrier that protects the brain and spinal cord parenchyma from the changeable milieu in the blood stream.[6]

Research in the field of autoimmune neuro-inflammation has provided insight into the extravasation of activated CD4$^+$ T cells across the BBB. Here, the immune cells employ the integrins lymphocyte function-associated antigen (LFA)-1 (αLβ2, CD11a/CD18), macrophage-1 antigen (Mac)-1 (αMβ2, CD11b/CD18) and very late antigen (VLA)-4 (α4β1, CD49d/CD29).[7] The ligands of these integrins on the BBB belong to the family of immunoglobulin-like cell adhesion molecules. Three of them, namely intercellular adhesion molecule (ICAM)-1, ICAM-2 and vascular cell adhesion molecule (VCAM)-1 fulfil critical roles in immune cell extravasation.[8–10] Importantly, increased levels of ICAM-1 and VCAM-1 on the BBB occur during neuro-inflammatory conditions in vivo or can be induced by cytokine stimulation in vitro.[7]

Regarding the extravasation of melanoma cells, VLA-4 has been assigned a role for adhesive interaction with endothelial VCAM-1 and diapedesis across immortalized human dermal microvascular endothelial cells (HMEC-I), human umbilical cord vascular endothelial cells (HUVECs) or immortalized mouse endothelioma cells in vitro.[11–15] In vivo, targeting of VLA-4 in a mouse model for the formation of lung metastasis reduced lung metastatic colonization.[13,15] The expression of VLA-4 in situ on clinical specimen of human melanoma patients correlated with melanoma progression and metastasis formation.[16,17] Taken together, the VCAM-1/VLA-4 axis has been assigned a role in the formation of melanoma lung metastasis in the mouse and in clinical outcome in melanoma patients. However, the role of melanoma VLA-4 has not been addressed for breaching the BBB, and neither has the frequency of VLA-4 positive melanoma brain metastasis been previously examined.

In this study, we addressed the role of VLA-4 on mouse B16F10 melanoma cells, mouse B78chOVA melanoma cells and on a patient-derived human melanoma cell line for adhesive interaction with the BBB. To model the BBB, we took advantage from the well-established primary mouse brain microvascular endothelial cells (pMBMECs) that form a tight barrier in vitro and proved valuable for studying many aspects of effector T cell extravasation.[8,9,18–22] In vitro live cell imaging under physiological flow revealed shear resistant arrest of melanoma cells on pMBMECs. Stimulation of pMBMECs with IL-1β strongly increased melanoma cell shear resistant arrest.

A comparison of melanoma cells with effector T cells revealed that similar expression of VLA-4 translated into similar arrest on the BBB but different post-arrest behavior: Immediately after arrest, effector T cells polarize, crawl and diapedese, whereas the melanoma cells remained without such obvious spatiotemporal dynamic probing of the BBB.[8,9] Importantly, shear resistant arrest of melanoma cells was completely abrogated by antibody blockade of VLA-4. Employing a tissue microarray (TMA) constructed from human brain resection or autopsy specimen, we revealed that the majority of melanoma brain metastasis, namely 92%, stained positive for VLA-4. We hypothesized on a delayed but critical role of VLA-4 for melanoma cell extravasation. Indeed, live cell imaging over hours revealed melanoma cell intercalation into the tight monolayer formed by pMBMECs. Intercalation was severely increased upon inflammatory conditions of the pMBMECs. An important finding of our study is the dramatic reduction of melanoma cell intercalation upon functional ablation of VLA-4. In line, melanoma cell-induced barrier break down of pMBMECs was significantly attenuated upon CD49d blockade. We conclude that VLA-4 on melanoma cells increases the risk of brain metastasis. In the context of personalized medicine, targeting VLA-4 on VLA-4 positive metastatic melanoma would interfere with brain metastasis formation.

Material and methods

Antibodies, cytokines and recombinant proteins

The rat anti-mouse antibodies to CD49d (PS/2), CD11a (FD441.8), CD49d/Itgb7 (DATK32), VCAM-1 (6C7.1), ICAM-1 (YNI/1.7) and the control antibody targeting human CD44 (9B5) were described before.[23,24] The hybridoma supernatant containing mouse anti-human antibody to CD49d (HP2/1) was kindly provided by Professor Francisco Sánchez-Madrid (Universidad Autónoma de Madrid, Spain) and has been previously described.[25] For function blocking of living human melanoma cells, purified HP2/1 and the respective mouse control antibody were from antibodies-online GmbH (Aachen, Germany). For immunohistology of paraffin-embedded human brain melanoma specimen, we used polyclonal rabbit anti human CD49d from AbD Serotec (AHP1225, BioRad Laboratories Inc). Recombinant murine TNF-α was from PromoKine (Vitaris AG, Baar, Switzerland) and recombinant murine IL-1β was from PeproTech (Rocky Hill, NJ, USA). Recombinant mouse or human ICAM-1/CD54 and mouse or human VCAM-1/CD106 Fc Chimera were from R&D Systems (Minneapolis, MN, USA).

Cells

pMBMECs. Isolation and culture of pMBMECs were performed as described before.[18,19] Brains of wild type or LifeAct-GFP mice in the C57BL/6 J background were used to isolate pMBMECs.[26] All animal procedures were performed in accordance with the Swiss legislation on the protection of animals under the approval BE72/15 issued by the veterinary office of the Canton Bern, Switzerland. The experiments have been conducted and reported in compliance with the ARRIVE guidelines. Immediately after isolation, pMBMECs were seeded into the appropriate culture vessel for experiments, i.e. pMBMECs were used without any passaging. Cytokine stimulation of pMBMECs was with TNF-α at 10 ng/ml or IL-1β at 20 ng/ml for 16 to 20 h followed by two washes (HBSS, 10 mM HEPES, 5% CS) to remove all cytokines prior to the experiment.

Brain endothelioma cells bEnd.5. The bEnd.5 mouse brain endothelioma cell line and culture conditions were described before.[19,27] All experiments were performed with bEnd.5 between passages 15 and 25.

Human melanoma cells. The human melanoma cell lines hMel-CD49d^{low} and hMel-CD49d^{high} were established and cultured as described before.[28] These patient-derived melanoma cell lines were obtained from the University Research Priority Program (URPP) in translational cancer research biobank at the University of Zurich Hospital and corresponded to a VLA-4 high expressing culture (M140719) and a VLA-4 low expressing culture (M140625). These lines were derived from surplus material from consenting patients (EK647/800) according to previously published protocols and characterized for VLA-4 expression according to approval from the local institutional review board (KEK-ZH.NR2014-0425).[28] For experiments, hMel-CD49d^{low} and hMel-CD49d^{high} were used between passages 6 and 15.

Mouse melanoma cells. Mouse melanoma B78chOVA cell line is a mCherry red fluorescent protein (RFP) expressing derivate of the B78 cell line and was kindly provided by Professor Matthew Krummel (University of California, San Francisco, USA).[29] The mouse melanoma cell lines B78 and B16F10 are derivates of the mouse melanoma cell line B16 and cultured as published.[29–31] Prior to the experiments, B16F10 and B78chOVA cells were expanded such that all experiments could be done with cells differing not more than five rounds of passaging.

Effector/memory T cells. For in vitro experiments with activated effector T cells, the proteolipid protein (PLP) peptide aa139–153 specific CD4$^+$ Th1 effector/memory cell line SJL.PLP7 was stimulated prior to experiments with their cognate antigen as described.[9,24]

Flow cytometry

For detachment of human or mouse melanoma cells, EDTA containing wash buffer (HBSS, 10 mM HEPES, 5 mM EDTA) was used. Then, cells were washed once with flow cytometry buffer (PBS, 2.5% FBS, 0.1% NaN$_3$) and aliquoted at $0.5 - 1 \times 10^6$ cells per well in a 96 round bottom well plate. Antibody incubation was performed for 30 min with primary antibodies and with PE-conjugated secondary antibodies at 4°C with washing steps in between and followed by fixation in 1% PFA/PBS. For measurement the FACSCalibur (BD Biosciences, San Diego, CA), and for analysis the FlowJo software (Tree Star Ashland, OR) were used.

Quantitative polymerase chain reaction

Total RNA was extracted from melanoma or T cells using High Pure RNA Isolation Kit (ROCHE, Basel, Switzerland). RNA samples (10 ng) were reverse transcribed into cDNA using random hexamer primers and the Super Script III First Strand cDNA Synthesis kit (Invitrogen^{TM}, Life Technologies). Real-time PCR was performed using MesaGreen qPCR Master Mix Plus for SYBR Assay low ROX (Eurogentec S.A., Seraing, Belgium) using an Applied Biosystems ViiA 7 machine (Life Technologies^{TM}). Primers (Eurogentec S.A.) were as follows. Mouse CD49d (NM 010576) GGTCAATCCTGGGGCGATTT (sense)/CCAGGC ATGTCTTCCCACAA (reverse) and mouse ribosomal protein S16 (Rps16) (the endogenous control) (NM 013647) GATATTCGGGTCCGTGTGA (sense)/TTG AGATGGACTGTCGGATG (reverse) or human CD49d (NM 000885) pair 1 AAGAATCCCGGC CAGACGTG (sense)/CTGGCTGTCTGGAAAGT GTGA (reverse), pair 2 TGGACTGGCTCTCTTTTT GTCTA (sense)/GGTAGTATGCTGGCTCCGAAA (reverse), pair 3 CTCTACATGTCAAACTACCC GTG (sense)/GTCAAGTTGTACCACGCCAG (reverse) and human ribosomal protein S16 (Rps16) (endogenous control) (NM 001020) CTGGAGATGA TTGAGCCGCG (sense)/CGGATAGCATAAATCT GGGCC (reverse).

Melanoma cell binding to immobilized proteins under static conditions

For detachment of human or mouse melanoma cells, EDTA containing wash buffer (HBSS, 10 mM HEPES, 5 mM EDTA) was used. After centrifugation, melanoma cells were suspended in migration assay medium

(MAM) (DMEM, 25 mM HEPES, 5% CS, 4 mM L-Glutamine) adjusted to 1×10^6 cells/ml; 12-well diagnostic microscope slides (Life Technologies, ThermoFisher) were coated with recombinant mouse ICAM-1/Fc (mICAM-1) or VCAM-1/Fc (mVCAM-1) proteins (R&D Systems, Abingdon, UK) as published before.[8,9] Each pre-coated well was overlaid with 20 µl cell suspension. Slides were kept on a tilting platform for 15 min at room temperature. Afterwards, two washing steps in PBS removed non-bound melanoma cells. Then slides were placed in a jar with 2.5% glutaraldehyde for fixation for 2 h and mounted with Mowiol. Images were acquired using an AxioObserverZ.1 microscope (Carl Zeiss AG, Feldbach, Switzerland) with the $10\times$ objective (Plan-Neofluar, $10\times/0.3$, Carl Zeiss AG) and the AxioCam.MRm camera (Carl Zeiss AG). Evaluation was performed by counting bound cells per field of view (FOV) with three FOVs per well.

Diapedesis experiment

Diapedesis of T cells across bEnd5 was performed as described before.[27] In brief, 10^5 T cells were added to the upper chamber. After a migration period of 4 h, T cells that were diapedesed across the bEnd5 were collected from the lower chamber. Diapedesis of melanoma cells differed due to the lower migration speed and adhesive character of melanoma cells in the following points: 1. Costar Transwell® filters with 8 µm pores instead of 5 µm pores grown with bEnd5 were used. 2. The migration period was 24 h instead of 4 h. 3. Melanoma cells were starved for 24 h prior to the experiment in culture medium without FCS. 4. Migration was towards MAM containing 10% FCS in the lower chamber. 5. Diapedesed melanoma cells remained adherent to the lower face of the filter. To count melanoma cells, filter inserts were fixed with formaldehyde (3.7% in PBS) for 30 min, washed with PBS and stained with phalloidin-FITC (0.33 µg/ml) and DAPI (1 µg/ml) in PBS with 0.5% BSA and 0.1% Triton-X 100. Stained filters were mounted with Mowiol and imaged using a Nikon Eclipse E 600 microscope equipped with a Nikon Digital Camera at $20\times$. Diapedesed melanoma cells were counted from four images, each covering a surface of 0.278 mm². For comparison with T cell diapedesis, numbers of diapedesed melanoma cells were extrapolated to the full surface area of the filter of 0.3 cm².

In vitro live cell imaging

For all imaging experiments, the AxioObserverZ.1 microscope (Carl Zeiss AG, Feldbach, Switzerland) was used. Magnification was at $10\times$ (Objective Plan-Neofluar, $10\times/0.3$, Carl Zeiss AG), illumination for

RFP or GFP fluorescence was with light emitting diodes (Carl Zeiss AG) and image acquisition was with the AxioCam.MRm camera (Carl Zeiss AG). Images were acquired at intervals and for a total period as indicated. Image processing was with the ZENblue software (Carl Zeiss AG) and ImageJ (National Institute of Health, Bethesda, MD, USA).

Melanoma cell shear resistant arrest on recombinant proteins or on pMBMECs. In vitro live cell imaging of shear resistant arrest and behavior of melanoma cells on pMBMECs under physiological flow was adapted from our previously described experiments using CD4$^+$ effector T cells.[8,32] Melanoma cells were detached with EDTA containing wash buffer (HBSS, 10 mM HEPES, 5 mM EDTA) followed by centrifugation and resuspension in wash buffer (HBSS, 10 mM HEPES) at 2×10^6 cells/ml. At start of the experiment, melanoma cells were diluted in MAM at 1×10^6 cells/ml. Where indicated, melanoma cells have been incubated with a blocking antibody to mouse or human CD49d (PS/2 or HP2/1) or respective control antibodies at 10 µg/ml 15 min prior to the experiment. For analysis of shear resistant arrest, melanoma cells were perfused over a confluent monolayer of pMBMECs or immobilized recombinant proteins through a custom made flow chamber at 1×10^6 cells/ml. An initial accumulation of melanoma cells at 0.1 dyn/cm² for 3 or 4 min (negative time) was followed by physiological shear at 1.5 dyn/cm² (positive time). Shear resistant arrest of melanoma cells was determined 30 s after onset of physiological shear.

CD4$^+$ T cell dynamic interaction with pMBMECs under flow. In vitro live cell imaging of the dynamic interaction between CD4$^+$ effector T cells and pMBMECs under physiological flow was exactly as described before.[8,32]

Melanoma cell intercalation. pMBMECs were isolated from C57BL/6 LifeAct-GFP mice and grown to a confluent monolayer in a flat-bottom 96-well plate.[26] 16 to 20 h prior to the experiment, pMBMECs were either stimulated with cytokine or left unstimulated. To start the experiment, pMBMECs were washed twice with CS containing wash buffer (HBSS, 10 mM HEPES, 5% CS) and overlaid with 100 µl MAM containing control or VCAM-1 blocking antibody at 20 µg/ml. Mouse melanoma cells were collected by detachment using EDTA containing wash buffer (HBSS, 10 mM HEPES, 5 mM EDTA) and centrifugation. Then, the cell pellet was resuspended in PBS, 0.1% BSA at 0.5×10^6 cells/ml and incubated with control or CD49d blocking antibody at 20 µg/ml for 10 min. Then, 100 µl of melanoma cell suspension (5×10^4

cells) was added into each well with pMBMECs. Time lapse imaging was started 25 min after addition of melanoma cells taking an image every 5 min. In this experiment, B78chOVA melanoma cells and pMBMECs were clearly identifiable through their mCherry or GFP fluorescent signal, respectively. Intercalation became visible through displacement of the GFP signal from pMBMECs. Evaluation of intercalation was done by counting sites of displaced pMBMECs.

TMA and immune-histochemical staining

To assess CD49d in brain metastases of malignant melanomas, we constructed a TMA with resection or autopsy samples from 65 patients as previously described.[33] Three spots each were taken for surgical specimens and two spots per metastasis for autopsy cases. Human thymus was used as positive control. TMA construction and immune-histochemical analysis were performed with approval of the Ethics Committee of the Canton of Bern (KEK 200/14). CD49d immunostaining was performed with rabbit anti human CD49d (AHP1225, BioRad Laboratories Inc.) at a concentration of 30 µg/ml using citrate buffer for antigen retrieval. Visualization was done with the Bond Polymer Refine Detection kit (Biosystems Switzerland AG, Muttenz, Switzerland) for 15 min. Two consecutive sections of the TMA were stained with eosin and hematoxylin to identify tumor cells or immune stained to identify CD49d positive tumor cells, respectively. CD49d expression was scored as described by Brachtl et al.[34] In short, samples with >30% positive tumor cells were classified as CD49d high, samples with <30%, but >1% positive tumor cells were classified as CD49d low and samples with <1% positive tumor cells were classified as CD49d negative. TMA spots that contained less than 50 well-preserved tumor cells were excluded from analysis.

Transendothelial electrical resistance

pMBMECs were grown to a confluent monolayer on filter inserts (0.4 µm pore size, ThinCert™, Greiner Bio-One, Vitaris AG, Baar, Switzerland). Impedance transendothelial electrical resistance (TEER) measurements (CellZscope®, Nanoanalytics, Muenster, Germany) were started three days after seeding according to the manufacturer's instructions. Assessment of pMBMEC barrier disruption by melanoma cells was started six to eight days after seeding, when TEER has developed.[8] Mouse melanoma cells were collected by detachment using EDTA containing wash buffer (HBSS, 10 mM HEPES, 5 mM EDTA) and centrifugation. T cells were collected by centrifugation. Then, cell pellets were resuspended in PBS, 0.1% BSA at 2.5×10^6

cells/ml (concentration A) or 2.0×10^5 cells/ml (concentration B) and if needed incubated with control or CD49d blocking antibody at 20 µg/ml for 10 min. Then, 20 µl or 4 µl of concentration A with 5×10^4 and 1×10^4 cells, respectively, or 10 µl of concentration B with 2×10^3 cells was added into each well with pMBMECs. For B16F10 melanoma cell conditioned medium, supernatant was harvested from a confluent B16F10 cell culture plate grown for 48 h without medium change. TEER measurement was started immediately with one measurement per hour.

Statistical evaluation

Differences between two groups were analyzed by the unpaired Student t-test using GraphPad Prism 6.0 software (Graphpad software, La Jolla, CA, USA). If not stated differently, error bars show standard error of the mean and experiments have been executed three times in triplicates at the least. Asterisks indicate significant differences (*$p < 0.05$, **$p < 0.01$, and ***$p < 0.001$). Blinding during data analysis has not been done.

Results

Mouse B16F10 melanoma cells adhere to the inflamed BBB under physiological flow

One important step in the formation of melanoma brain metastasis is the initial contact formation between the circulating metastatic melanoma cell and the ECs of the BBB. In a first step, we asked whether mouse melanoma cells would form adhesive cell–cell interaction with the BBB under physiological flow conditions. Experimentally, we employed a flow chamber setup combined with in vitro live cell imaging to analyze B16F10 melanoma cell arrest on primary mouse brain microvascular endothelial cells (pMBMECs). This model is well established for studying multiple aspects of leukocyte extravasation across the BBB.[19,32,35,36] Indeed, B16F10 melanoma cells achieved shear resistant arrest on pMBMECs (Figure 1(a) and (b)) (Supplementary Movie 1). Strikingly, arrest of B16F10 cells on IL-1β stimulated pMBMECs was significantly increased compared to unstimulated pMBMECs (Figure 1(a) and (b)) (Supplementary Movie 1). Thus, melanoma cells can bind to the BBB in a blood flow resistant manner and this adhesion to the BBB is significantly stronger in simulated inflammatory conditions.

Stimulation of pMBMECs with inflammatory cytokines such as TNF-α or IL-1β induces high levels of ICAM-1 and VCAM-1 and promotes the extravasation of CD4+ effector T cells.[8,9] In this study, a side-by-side comparison of the adhesive interaction of B16F10
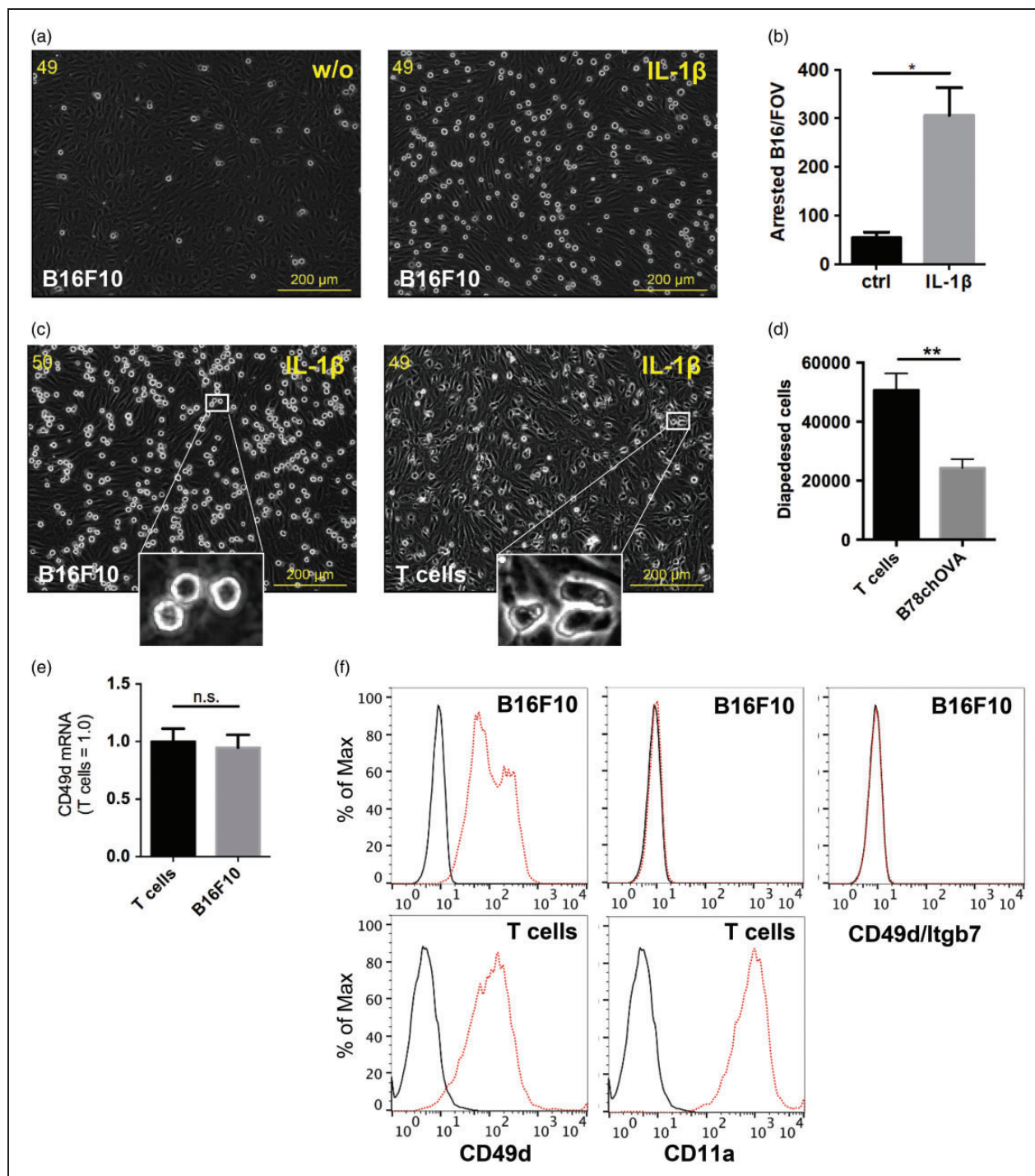
Figure 1. Shear resistant arrest of melanoma cells or CD4^{+} effector T cells on the BBB. (a) Shear resistant arrest of B16F10 mouse melanoma cells on unstimulated (left, w/o) or IL-1β stimulated (right, IL-1β) pMBMECs. Images were selected from a time lapse imaging experiment and show melanoma cells that resisted detachment by physiological flow at 1.5 dyn/cm^2. Numbers 49 or 50 indicate seconds past onset of physiological flow. An additional movie file shows this in more detail (see Supplementary File 1). (b) Statistical evaluation of (a) showing the mean of three experiments per condition. (c) Shear resistant arrest of B16F10 mouse melanoma cells (left) or activated CD4^{+} T cells (right) on IL-1β stimulated pMBMECs. Inserts delineate different cellular morphology of melanoma versus T cells. An additional movie file shows this in more detail (see Additional File 2). (d) Diapedesis of activated CD4^{+} T cells or B78chOVA melanoma cells across TNF-α stimulated brain endothelial cells bEnd.5. Values are the mean of at least four different experiments performed in triplicates. Please note the different migration periods, which was 4 h for T cells and 24 h for B78chOVA melanoma cells. (e) Quantitative PCR comparing mRNA level of CD49d of T cells (set to 1.0) to B16F10 melanoma cells. (f) Flow cytometry of B16F10 (upper panels) or CD4^{+} T cells (lower panels). Black lines, isotype control. Red lines, target antigens (left, CD49d; center, CD11a; right CD49d/Itgb7).

melanoma cells or CD4^{+} effector T cells with the stimulated BBB showed similar shear resistant arrest but differences in the dynamic behavior of the adherent cells (Figure 1(c)) (Supplementary Movie 2). B16F10 melanoma cells remained roundish and rather immobile while adhering on the pMBMECs, whereas spreading, polarization, crawling and diapedesis of CD4^{+} effector T cells occurred in the very same timeframe (Figure 1(c)) (Supplementary Movie 2). We also compared diapedesis of CD4^{+} effector T cells to the diapedesis of B78chOVA melanoma cells across brain endothelium in a static two chamber based setup. Due to the very different speed of migration, B78chOVA cells were allowed to diapedese for a period of 24 h compared to a T-cell migration period of only 4 h. Still, significantly less melanoma cells diapedesed across the endothelial layer (Figure 1(d)). We have previously demonstrated important roles for the integrins LFA-1, a binding partner of ICAM-1, and VLA-4, a binding partner of VCAM-1, on CD4^{+} effector T cells for dynamic adhesive contact with the BBB.[9] Therefore, we asked whether B16F10 cells express LFA-1 and VLA-4 similar to CD4^{+} effector T cells. Quantitative real-time polymerase chain reaction (qRT-PCR) revealed comparable expression of CD49d mRNA in B16F10 melanoma cells and CD4^{+} effector T cells (Figure 1(e)). Flow cytometry confirmed cell surface expression of CD49d on B16F10 melanoma cells comparable to CD4^{+} effector T cells (Figure 1(f)). Since flow cytometry showed complete absence of the α4/β7-integrin heterodimer by a heterodimer specific antibody, we concluded that all CD49d form part of VLA-4. Flow cytometry further revealed that B16F10 melanoma cells were devoid of LFA-1, whereas CD4^{+} effector T cells expressed LFA-1 (Figure 1(f)). We concluded that comparable expression of VLA-4 by CD4^{+} effector T cells and B16F10 does not translate to a similar mechanism of diapedesis.

VLA-4 mediates shear resistant adhesion of mouse melanoma cells to the BBB

Endothelial ICAM-1 and VCAM-1 are important players in the extravasation of CD4^{+} effector T cells across the BBB in vitro and in vivo.[8–10,37–39] Since B16F10 express VLA-4 but not LFA-1, we hypothesized that their adhesive interaction might be mediated through endothelial VCAM-1 but not ICAM-1. To test this hypothesis, we performed in vitro live cell imaging of anti-CD49d, anti-CD11a, or control treated B16F10 melanoma cell interaction with IL-1β-stimulated pMBMECs under flow conditions (Figure 2(a)) (Supplementary Movie 3). Shear resistant arrest of B16F10 melanoma cells was completely abrogated by

blocking CD49d, whereas the anti CD11a or isotype control antibodies remained without effect on shear resistant arrest of B16F10 melanoma cells to the IL-1β stimulated pMBMECs (Figure 2(b)) (Supplementary movie 3). To verify the critical role of endothelial VCAM-1 as the endothelial ligand, we performed binding assays with recombinant ICAM-1 and VCAM-1. Fibronectin and BSA were also tested as positive and negative controls, respectively. We observed high numbers of B16F10 cells bound to recombinant VCAM-1 or fibronectin, whereas binding to BSA or recombinant ICAM-1 was absent (Figure 2(c)). In vitro live cell imaging confirmed shear resistant arrest of B78chOVA melanoma cells to recombinant VCAM-1 but not to ICAM-1 (Figure 2(d)). Finally, the role of VLA-4 for the adhesion to recombinant VCAM-1 under physiological flow was verified by the complete blockade of melanoma cell shear resistant arrest through the anti-CD49d antibody (Figure 2(e)). Taken together, our data substantiated the prominent role of VLA-4 on circulating metastatic melanoma cells for arrest on the BBB via binding to endothelial VCAM-1.

VLA-4 is prominent on human melanoma brain metastases in situ

Having proven the important role of VLA-4 on mouse melanoma cells to initiate extravasation, i.e. to firmly adhere to the BBB, we asked whether CD49d is expressed in situ in melanoma brain metastasis of human patients. To this end, we constructed a TMA from brain tissue resections and brain autopsies of melanoma patients with brain metastasis. Two consecutive sections were cut and stained with eosin and hematoxylin to identify tumor cells or immune-stained to detect CD49d, respectively (Figure 3). The immunostaining was scored as described by Brachtl et al.,[34] i.e. melanoma with >30% positive tumor cells were classified as VLA-4 high, melanoma with <30%, but >1% positive cells were classified as VLA-4 low and tumors with <1% stained tumor cells were classified as VLA-4 negative. TMA spots that contained less than 50 well-preserved tumor cells were excluded from analysis. Normal appearing brain tissue and thymus were used as controls in the immunostaining (Figure 3). Out of 50 melanoma brain metastases evaluated, 31 (62%) were CD49d high, 15 (30%) were CD49d low and 4 (8%) were CD49d negative (Table 1). We found minimal intra-tumoral heterogeneity regarding the CD49d immune-reactivity (data not shown). Only two metastases showed clear differences between different tumor spots; in both cases, one spot each had CD49d high and CD49d low expression, respectively. In summary, the high fraction of 92% of CD49d positive brain
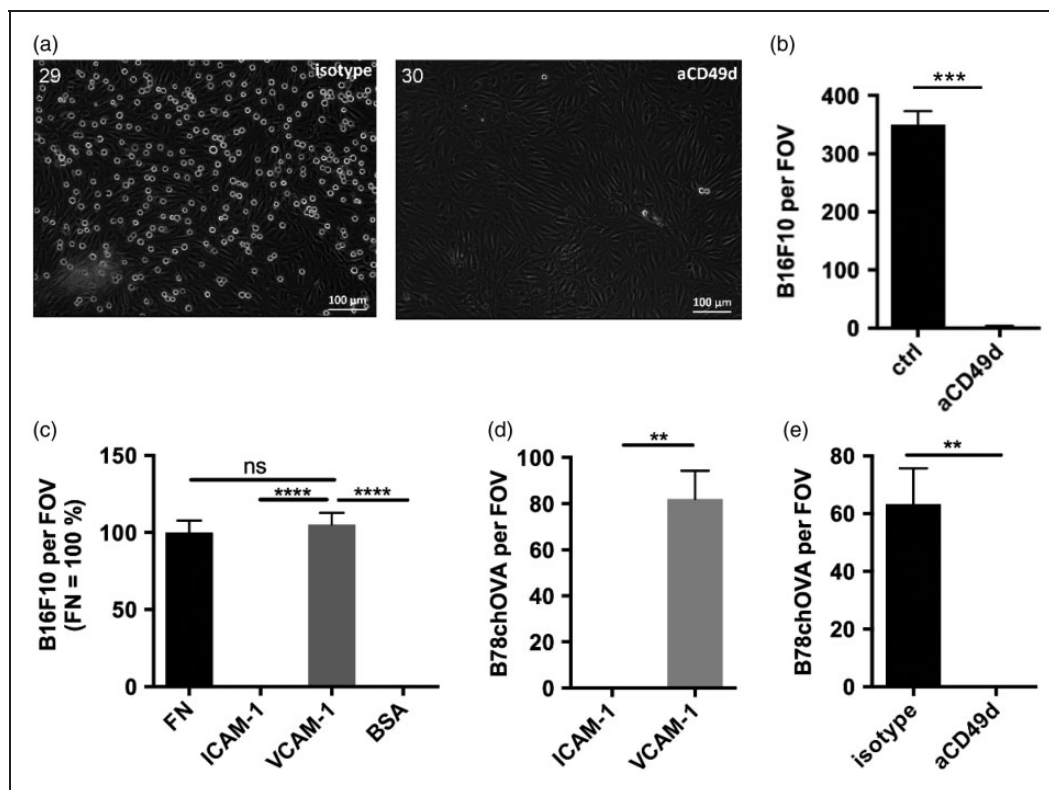
Figure 2. CD49d binding to VCAM-1 mediates shear resistant arrest of mouse melanoma cells on the BBB. (a) Shear resistant arrest of mouse B16F10 melanoma cells on IL-1β stimulated pMBMECs after 29 (left) or 30 (right) seconds at 1.5 dyn/cm². Melanoma cells were treated with the isotype control antibody (left) or with anti CD49d antibody (right). An additional movie file shows this in more detail (see Additional File 3). (b) Quantitative evaluation of (a). (c) Binding of mouse B16F10 melanoma cells to fibronectin (FN), ICAM-1, VCAM-1 or BSA under static conditions. Representative experiment performed in triplicates at least. (d) Shear resistant arrest of B78chOVA mouse melanoma cells on ICAM-1 or VCAM-1. (e) Shear resistant arrest of B78chOVA mouse melanoma cells on VCAM-1 after treatment with an isotype antibody or an antibody blocking CD49d (aCD49d). (b–e) Three or more experiments per condition.

metastases highlights the presumptive role of VLA-4 in the formation of melanoma brain metastasis.

VLA-4 mediates shear resistant adhesion of human melanoma cells to the BBB

So far, we have shown the important role of VLA-4 for mouse B16F10 melanoma cell shear resistant adhesion to endothelial VCAM-1 and we have revealed a predominance for CD49d positive melanoma metastasis in the brain. Hence, we hypothesized that VLA-4 might have similar functions in human and mouse melanoma cells. To test this, we selected two human melanoma cell lines (hMel) with either very low (hMel-CD49d^low) or high (hMel-CD49d^high) CD49d expression, as determined in flow cytometry and quantitative polymerase chain reaction (qPCR) (Figure 4(a) and (b)). As expected, different CD49d levels corresponded to respectively higher binding to recombinant

human VCAM-1 of hMel-CD49d^high cells compared to hMel-CD49d^low cells (Figure 4(c)). Consistently, binding of hMel-CD49d^high cells to VCAM-1 was blocked completely by the anti-human CD49d antibody HP2/1 (Figure 4(d)).[25] hMel-CD49d^high cells did not bind to recombinant human ICAM-1 or BSA (Figure 4(d)). This provided further proof for the specificity of the adhesive interaction of VLA-4 to VCAM-1. Next, we tested shear resistant arrest of hMel-CD49d^high cells on pMBMECs in in vitro live cell imaging under flow. Efficient binding of human VLA-4 to mouse VCAM-1 is well established and has been published before.[39,40] hMel-CD49d^high cells showed increased shear resistant arrest on IL-1β stimulated pMBMECs compared to unstimulated pMBMECs (Figure 4(e)). Antibody blockade of CD49d completely abrogated shear resistant arrest of hMel-CD49d^high cells on IL-1β stimulated pMBMECs (Figure 4(f)). Taken together, expression of VLA-4 by metastatic human

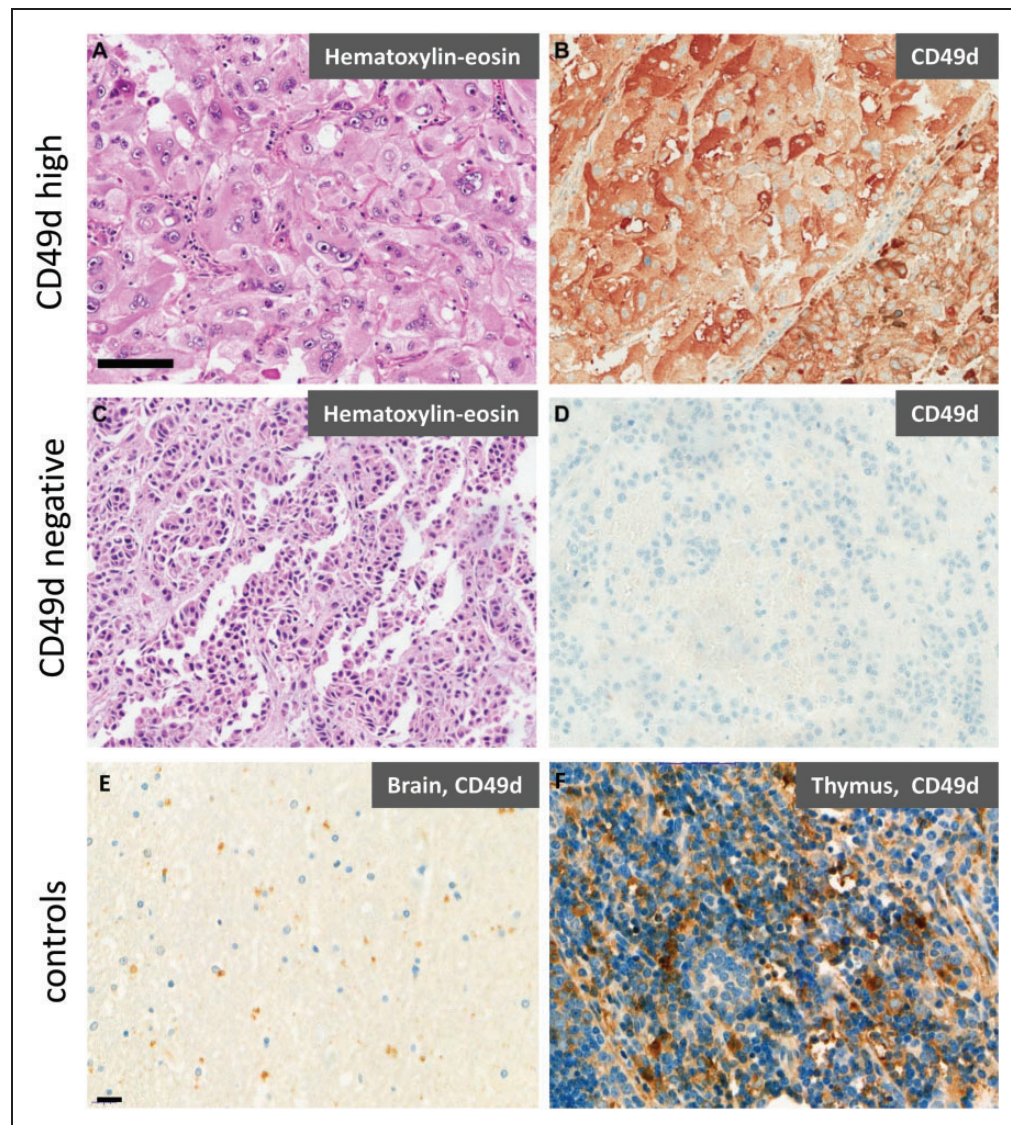**Figure 3.** CD49d on human melanoma brain metastases in situ. Custom-made tissue microarray (TMA) from human melanoma brain metastasis (38 biopsies from 38 patients, 12 autopsies from multiple metastasis of 3 patients). Tissue blocks were grouped according to their high, low or negative staining for human CD49d protein expression. (a, b) Example of CD49d-high melanoma metastasis. In this example, all tumor cells are strongly immunoreactive. (c, d) Melanoma metastasis negative for CD49d. (e) Non-affected brain tissue. (f) Thymus, positive control. (a, c) Hematoxylin–eosin. (b, d–f) CD49d immunostaining. Scale bars: (a) 100 μm, valid also for b–d. (e) 20 μm, valid also for f.

melanoma cells translated into shear resistant adhesive interaction of melanoma cells with VCAM-1 on the BBB.

VLA-4 mediates melanoma cell intercalation into the BBB

To further study the role of VLA-4/VCAM-1 interaction in pMBMEC barrier disruption by melanoma cells, we performed in vitro live cell imaging in a multi-well format over time. Here, we used B78chOVA melanoma cells due to their mCherry fluorescent protein expression and pMBMECs isolated from LifeAct-GFP mice allowing for unambiguous identification of mCherry positive melanoma cells and GFP positive pMBMECs.[26,29] Indeed, melanoma cells "merged" into the endothelial monolayer over time (Figure 5(a)). Overlays of phase contrast (all cells), mCherry (melanoma cells) and GFP (ECs) channels delineated that melanoma cell intercalation is initiated by displacement of the ECs followed by a dynamic melanoma cell spreading into the endothelial layer. An additional movie file shows this in detail (Supplementary Movie 4).
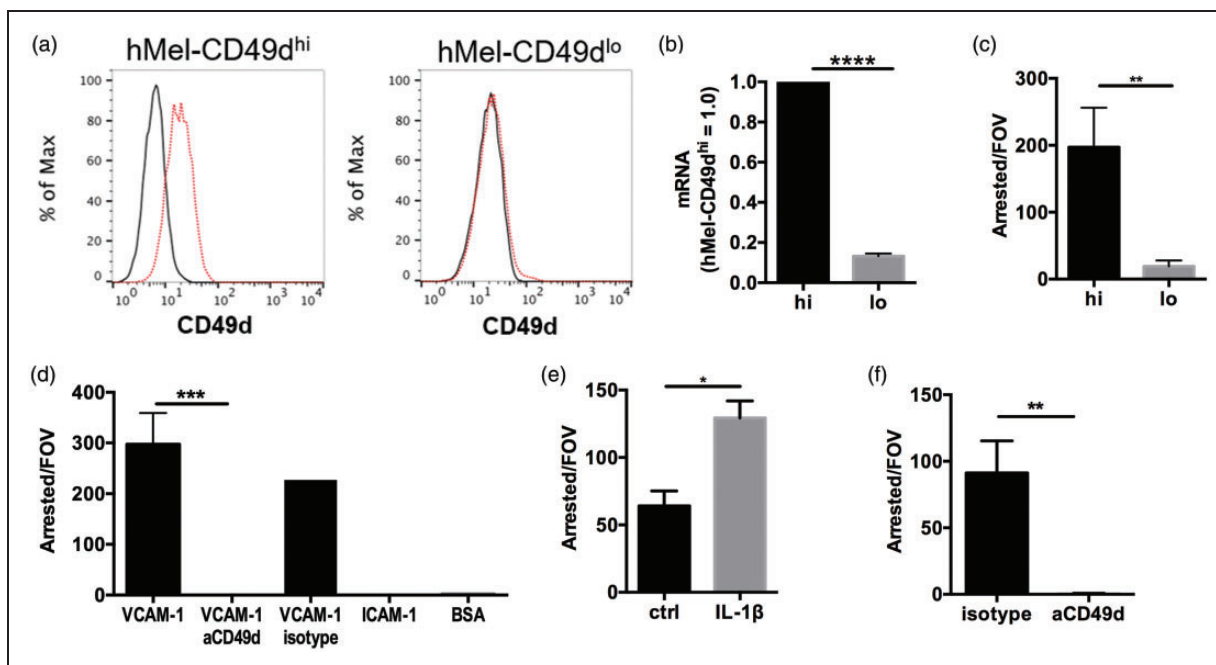
Figure 4. CD49d on human melanoma cells translates into increased adhesiveness to the BBB. (a) Flow cytometry of two human melanoma cell lines with either high CD49d (left, hMel-CD49d^{hi}) or low CD49d (right, hMel-CD49d^{lo}) expression. Black lines, isotype control. Red lines, anti CD49d. (b) Quantitative PCR comparing mRNA level of CD49d in hMel-CD49d^{hi} (hi, set to 1.0) to hMel-CD49d^{lo} (lo). (c) Shear resistant arrest of hMel-CD49d^{hi} (hi) and hMel-CD49d^{lo} (lo) on VCAM-1. (d) Shear resistant arrest of hMel-CD49d^{hi} to VCAM-1, ICAM-1 or BSA. Where indicated, hMel-CD49d^{hi} was treated with an antibody blocking CD49d (aCD49d) or isotype control (isotype). (e) Shear resistant arrest of hMel-CD49d^{hi} melanoma cells on unstimulated (ctrl) or IL-1β stimulated pMBMECs. (f) Shear resistant arrest of hMel-CD49d^{hi} melanoma cells on IL-1β stimulated pMBMECs after treatment with isotype control (isotype) or anti CD49d blocking antibody.

To address the role of VLA-4 and VCAM-1, pMBMECs and B78chOVA were pretreated with blocking anti VCAM-1 or anti CD49d antibodies, respectively. To account for increased adhesiveness of melanoma cells upon inflammatory conditions of the BBB, we also included unstimulated and TNF-α stimulated pMBMECs in this multi-well format experiment. Consistent with increased expression of VCAM-1 upon inflammation, we observed significantly more gap formation when pMBMECs were stimulated with TNF-α compared to the unstimulated pMBMECs (Figure 5(b) to (d)). Importantly, blockade of CD49d and VCAM-1 effectively reduced the numbers of gaps formed by the melanoma cells into unstimulated or stimulated pMBMECs compared to controls (Figure 5(b) to (d)). An additional movie file shows this in detail (Supplementary Movie 5). Thus, blockade of melanoma VLA-4 by anti CD49d and endothelial VCAM-1 by anti VCAM-1 had a strong beneficial effect on preserving the BBB.

VLA-4 contributes to BBB barrier disruption

Having demonstrated melanoma cell shear resistant arrest on the BBB followed by intercalation into the BBB, we hypothesized that melanoma cell intercalation would disrupt barrier properties. Indeed, fibrinogen deposition around the center of a human melanoma brain metastasis pointed to leakage of brain vessels in the progression of melanoma metastasis (Supplementary Figure 1). To target this observation experimentally, we measured TEER of pMBMECs exposed to various numbers of B16F10 melanoma cells over time (Figure 6(a)). We determined that 50,000 B16F10 melanoma cells induced a significant drop of TEER within only 1 h of co-culture without restoration of barrier properties after a period of 12 h (Figure 6(a)). Importantly, B16F10-conditioned medium did not compromise BBB barrier properties (Figure 6(b)). We further hypothesized that BBB break down is more severe upon melanoma co-culture compared to co-culture with CD4$^+$ effector T cells that crawl, probe and diapedese within minutes.[8,9] Indeed, pMBMEC barrier properties were significantly less compromised upon CD4$^+$ effector T cells co-culture compared to co-culture with B16F10 melanoma cells (Figure 6(b)). Finally, we hypothesized that ablation of VLA-4 would protect BBB barrier properties. For analysis, we treated B16F10 melanoma cells with anti
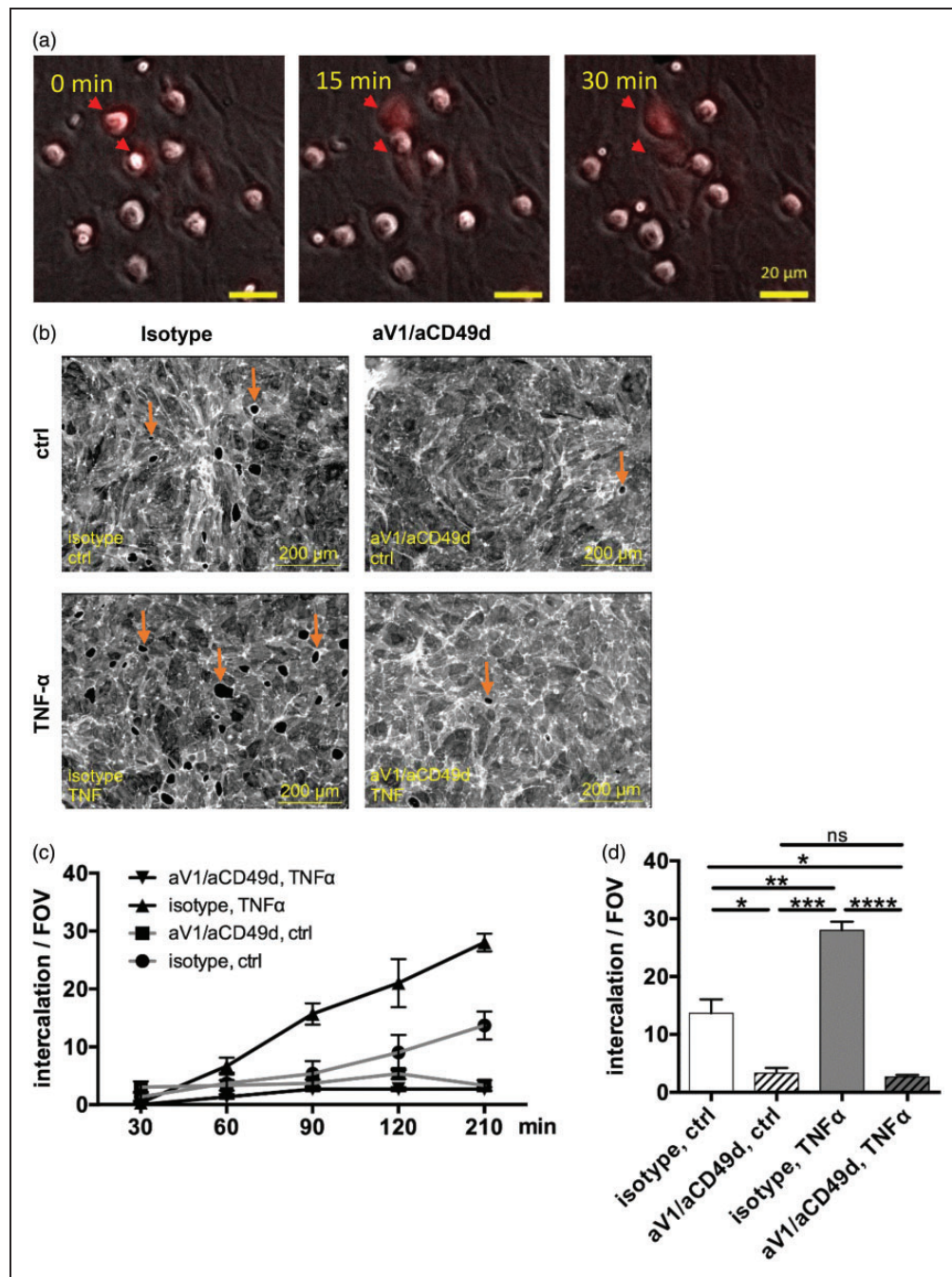
Figure 5. In vitro live cell imaging demonstrated the ultimate role of VLA-4/VCAM-1 for melanoma cell intercalation into the BBB. (a) Three consecutive microscopic images of two B78chOVA melanoma cells that intercalate into a monolayer of pMBMECs. Two intercalation events are depicted (arrowhead). 0 min, at the start of intercalation. 15 min, in the process of intercalation 15 min after start of intercalation. 30 min, intercalation is completed 30 min after start of intercalation. Overlay of the phase contrast channel (all cells) and the red fluorescent channel (B78chOVA). Images were taken with a 10× objective, scale bar 20 μm. An additional movie file shows this in more detail (Supplementary Movie 4). (b) Disruption of LifeAct-GFP pMBMECs by B78chOVA melanoma cells after 3 h. Some gaps in the pMBMECs are exemplarily marked with arrows. Ctrl, unstimulated pMBMECs. TNF-α, stimulated pMBMECs. B78chOVA and pMBMECs were left untreated (isotype) or were treated with anti CD49d or anti-VCAM-1 (aV1/aCD49d), respectively. Representative images 210 min after addition of B78chOVA melanoma cells to the pMBMECs are presented. Additional movie file shows this in more detail (Supplementary Movie 5). (c) Intercalation of B78chOVA melanoma cells into the pMBMEC layer over time. Numbers of gaps per FOV were counted at the time points indicated. One experiment performed in triplicates. (d) Statistical evaluation of B78chOVA melanoma cell intercalation at time point 210 min.
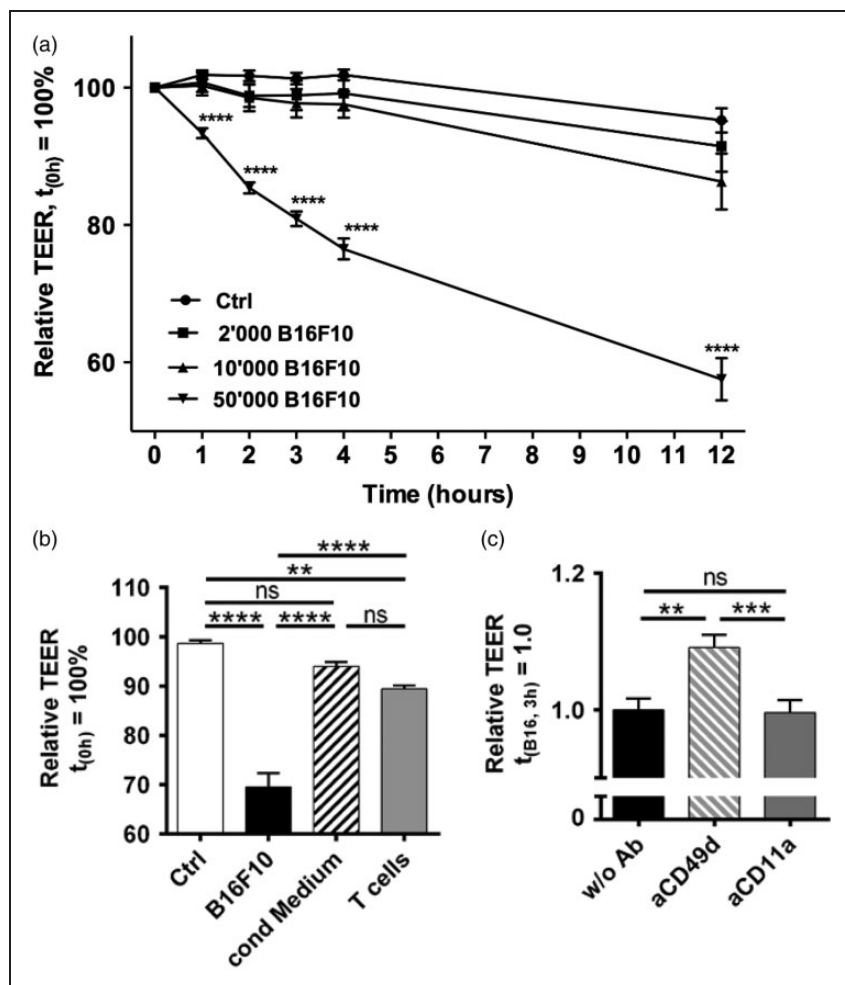
Figure 6. VLA-4/VCAM-1-mediated adhesion causes BBB barrier disruption by melanoma cells. (a) Relative TEER of pMBMECs without (ctrl) or with 2,000, 10,000 or 50,000 B16F10 melanoma cells over 12 h. The mean TEER of all samples at $t = 0$ (79.3 ± 4.64 Ω/cm^2) was set to 100%. (b) Relative TEER of pMBMECs without B16F10 melanoma cells (ctrl), with 50,000 B16F10 melanoma cells (B16F10), with melanoma-conditioned medium (cond medium) or with 50,000 CD4$^+$ T cells (T cells) after 3 h of measurement. Values are expressed in percent to TEER at $t = 0$, which was set to 100%. (c) Relative TEER of pMBMECs with B16F10 melanoma cells that remained untreated (w/o Ab), treated with the blocking anti CD49d antibody (aCD49d) or with the blocking anti CD11a antibody after 3 h of co-culture. TEER of pMBMECs co-cultured with untreated B16F10 was set to 1.0; the respective mean raw value was 63.6 ± 10.69 Ω/cm^2.

CD49d antibody or control antibody during co-culture with pMBMECs and measured TEER after 3 h. A significantly attenuated barrier disruption of pMBMECs by B16F10 melanoma cells upon antibody induced VLA-4 ablation compared to control corroborated our hypothesis (Figure 6(c)). Taken together, we have demonstrated that the VLA-4-mediated intercalation of metastatic mouse melanoma cells into the tight BBB translated into BBB barrier breakdown.

Discussion

In this study, we addressed the role of inflammation and VLA-4 expression for the interaction of melanoma cells with the BBB. Clearly, VLA-4-mediated

adhesiveness and intercalation were strikingly increased when the BBB was under simulated inflammatory conditions and thus ICAM-1 and VCAM-1 were expressed at high levels.[9,41] Increased adhesion of melanoma cells to cytokine stimulated non-BBB ECs has been described before.[42,43] From previous research, we know that ICAM-1 and VCAM-1 are important ligands for the extravasation of CD4$^+$ effector T cells across the inflamed BBB in vitro and contribute to the development of experimental autoimmune encephalomyelitis (EAE), which is an in vivo animal model of multiple sclerosis.[9,41] For extravasation, CD4$^+$ effector T cells exploit a highly dynamic interaction with the inflamed BBB, which has been demonstrated by in vitro live cell imaging or in vivo intravital

microscopy.[9,10,37,41] For comparison, we performed a comparison of melanoma cells with T cells adherent to the inflamed BBB. In remarkable contrast to the immediate dynamic behavior of the adherent CD4$^+$ effector T cells, melanoma cells retained a roundish cell shape and lacked immediate crawling and diapedesis. Moreover, the melanoma cells did not undergo adhesive interaction with ICAM-1. To visualize the diapedesis of melanoma cells, we had to extend imaging over several hours. This allowed us to observe the intercalation of melanoma cells into the BBB. Again, this process differs from the diapedesis of T cells that form a pore across the EC or open the EC junctions transiently and migrate through within minutes.[8] Diapedesis of CD4$^+$ effector T cells is completed within minutes and the endothelial monolayer seals immediately.[9,44] The differences in the mechanism of diapedesis were further manifested by the parallel comparison of BBB barrier properties, while in co-culture with T cells or melanoma cells: The more penetrative CD4$^+$ T effector cells significantly less compromised the barrier properties of the BBB compared to melanoma cells. Taken together, the comparable expression level of VLA-4 by B16F10 melanoma cells and CD4$^+$ effector T cells translates into similar adhesiveness to the BBB, while the mode of interaction with and the process of diapedesis across the BBB is very different.

Already in the 1990s, a role for VLA-4 was described in melanoma metastasis formation in the lung in vivo. In experimental animals that intravenously received melanoma cells, the treatment with blocking antibodies targeting VLA-4 or VCAM-1 reduced pulmonary foci formation, whereas the treatment with pro-inflammatory stimuli increased pulmonary foci formation.[45,46] Also based on intravenous injection of melanoma cells, more recent studies demonstrated reduced pulmonary foci formation upon genetic knockdown of VLA-4 expression in B16F10 melanoma cells or anti-VCAM-1 treatment after transfer of human melanoma cells into nude mice.[13,15] However, strikingly different results were obtained in an in vivo metastasis model in which melanoma cells were injected subcutaneously and thus must first intravasate into the vasculature before reaching the lung. Here, expression of VLA-4 on melanoma cells reduced pulmonary melanoma metastasis.[47] Presumably, VLA-4 fulfils diverse roles in different stages of melanoma metastasis formation. This assumption was also drawn by another previous study that showed inverse correlation between the invasiveness of melanoma and CD49d expression.[16] Maybe, CD49d in primary pre-metastatic tumors restrains melanoma cells from invasion.

Here, we elucidated the critical role of VLA-4 on melanoma cells for breaching the BBB. We investigated the role of VLA-4 in mouse melanoma cells and in human

Table 1. Number and percentage of CD49d positive (high or low) and negative samples on TMA.

	CD49d		
	High	Low	Negative
All metastases	31 (62%)	15 (30%)	4 (8%)
Resection specimen	25 (66%)	11 (29%)	2 (5%)
Autopsy specimen	6 (50%)	4 (33%)	2 (17%)

TMA: tissue microarray.

melanoma cells for adhesion to the BBB using in vitro live cell imaging with physiological flow. As an in vitro model of the BBB, we employed pMBMECs. In previous research, we have validated pMBMECs for the expression of tight junction molecules and formation of a BBB-like tight barrier.[18,19] Using this setup, we revealed a complete abrogation of melanoma cell shear resistant arrest on the BBB upon anti-VLA-4 treatment. Our results amend previous research describing a partial inhibition of melanoma cell adhesion to TNF-α stimulated bEnd.3 cells, a brain derived endothelioma cell line, or leptomeningeal cells upon antibody blockade of VCAM-1.[14,48] In addition, other studies describe partial inhibition of melanoma cell adhesion to non-BBB ECs upon treatment with anti VCAM-1 or anti CD49d antibody.[42,43] Possible reasons for the more stringent result of our study might have been the use of the barrier forming pMBMECs and the continuous application of flow. This particular setup might have excluded VLA-4 independent adhesion of melanoma cells to extracellular matrix proteins accessible through the permeable cell–cell junctions of brain endothelioma cells or non-BBB ECs.[19] Importantly, the blockade of VLA-4 completely abrogated melanoma cell intercalation into the BBB layer, even under cytokine-stimulated condition. Thus, our data reveal a hitherto unknown exclusive role for VLA-4 in the adhesive interaction of melanoma cells with the BBB.

By staining a TMA, we demonstrated a high prevalence for CD49d positive melanoma in human brain metastasis: 92% of tumors stained positive for CD49d. Effects of VLA-4 on the metastatic cascade of melanoma were shown in different melanoma cell lines in vitro before.[12] Moreover, melanoma cell lines with a higher invasiveness into human amnion expressed several fold higher levels of VLA-4 compared to the parental cell line.[49] Another study investigated integrin expression on human melanoma lesions and found that only 11% (2 of 18) non-tumorigenic lesions compared to 39% (9 of 23) tumorigenic neoplasms expressed CD49d.[50] Using Affymetrix® expression array data published in GeneOmnibus (GEO), we compared relative mRNA expression of CD49d in human

primary melanocytes with human melanoma brain metastasis and found a 5.42-fold increased expression of CD49d mRNA in the brain metastasis samples (Supplementary Figure 2). Considering further patient samples published in Schadendorf et al.[17] 63% of 59 primary cutaneous melanomas analysed were CD49d positive.[17] This, however, is remarkably different from the 92% CD49d positive melanoma in brain metastasis as determined in this study. Thus, our TMA data provide further evidence for the malignant character of CD49d expression in melanoma.

In the treatment of multiple sclerosis patients, the humanized anti-CD49d antibody natalizumab represents a validated medication that significantly reduces relapse rates by inhibiting pathological immune cell extravasation across the BBB.[51,52] Pharmaceutical targeting of VLA-4 on melanoma or lymphoma cells using the VLA-4 binding peptidomimetic ligand LLP2A is under pre-clinical investigations.[53–55] Our study led us to conclude that targeting VLA-4 on VLA-4 positive melanoma cells would interfere with brain metastasis formation. The selection of melanoma patients with aggressive and VLA-4-high metastasizing melanoma tumors for the treatment with a medication that functionally ablates VLA-4 could be a valid strategy in the context of personalized medicine.

Declaration of conflicting interests

The author(s) declared no potential conflicts of interest with respect to the research, authorship, and/or publication of this article.

Authors' contributions

AG-M, PZ, TG, CM performed and analysed experiments. FM, GE and JVS gave advice. ML provided the human biopsy derived material and gave advice. DF evaluated CD49d gene expression from GEO GSE 44660. EH designed the TMA and evaluated staining data. RL designed this project, performed and analysed experiments and wrote the manuscript.

Supplementary material

Supplementary material for this paper can be found at the journal website: http://journals.sagepub.com/home/jcb.

ORCID iD

Thomas Gruber http://orcid.org/0000-0001-5210-1995
Ekkehard Hewer http://orcid.org/0000-0002-9128-0364
Ruth Lyck http://orcid.org/0000-0002-6479-4837

References

1. Mangana J, Cheng PF, Kaufmann C, et al. Multicenter, real-life experience with checkpoint inhibitors and targeted therapy agents in advanced melanoma patients in Switzerland. *Melanoma Res* 2017; 27: 358–368.
2. Tas F. Metastatic behavior in melanoma: timing, pattern, survival, and influencing factors. *J Oncol* 2012; 2012: 647684.
3. Steeg PS. Targeting metastasis. *Nat Rev Cancer* 2016; 16: 201–218.
4. Saxena M and Christofori G. Rebuilding cancer metastasis in the mouse. *Mol Oncol* 2013; 7: 283–296.
5. Tamura A and Tsukita S. Paracellular barrier and channel functions of TJ claudins in organizing biological systems: advances in the field of barriology revealed in knockout mice. *Semin Cell Dev Biol* 2014; 36: 177–185.
6. Obermeier B, Verma A and Ransohoff RM. The blood-brain barrier. *Handb Clin Neurol* 2016; 133: 39–59.
7. Abadier M and Lyck R. Pathways across the blood-brain barrier. In: Lyck R and Enzmann G (eds) *The blood brain barrier and inflammation*. Cham: Springer International Publishing, 2017, pp.187–211.
8. Abadier M, Haghayegh Jahromi N, Cardoso Alves L, et al. Cell surface levels of endothelial ICAM-1 influence the transcellular or paracellular T-cell diapedesis across the blood-brain barrier. *Eur J Immunol* 2015; 45: 1043–1058.
9. Steiner O, Coisne C, Cecchelli R, et al. Differential roles for endothelial ICAM-1, ICAM-2, and VCAM-1 in shear-resistant T cell arrest, polarization, and directed crawling on blood-brain barrier endothelium. *J Immunol* 2010; 185: 4846–4855.
10. Bartholomaus I, Kawakami N, Odoardi F, et al. Effector T cell interactions with meningeal vascular structures in nascent autoimmune CNS lesions. *Nature* 2009; 462: 94–98.
11. Schlesinger M and Bendas G. Contribution of very late antigen-4 (VLA-4) integrin to cancer progression and metastasis. *Cancer Metastasis Rev* 2015; 34: 575–591.
12. Klemke M, Weschenfelder T, Konstandin MH, et al. High affinity interaction of integrin alpha4beta1 (VLA-4) and vascular cell adhesion molecule 1 (VCAM-1) enhances migration of human melanoma cells across

activated endothelial cell layers. *J Cell Physiol* 2007; 212: 368–374.

13. Tichet M, Prod'Homme V, Fenouille N, et al. Tumour-derived SPARC drives vascular permeability and extravasation through endothelial VCAM1 signalling to promote metastasis. *Nat Commun* 2015; 6: 6993.

14. Fritzsche J, Simonis D and Bendas G. Melanoma cell adhesion can be blocked by heparin in vitro: suggestion of VLA-4 as a novel target for antimetastatic approaches. *Thromb Haemost* 2008; 100: 1166–1175.

15. Schlesinger M, Roblek M, Ortmann K, et al. The role of VLA-4 binding for experimental melanoma metastasis and its inhibition by heparin. *Thromb Res* 2014; 133: 855–862.

16. Schadendorf D, Gawlik C, Haney U, et al. Tumour progression and metastatic behaviour in vivo correlates with integrin expression on melanocytic tumours. *J Pathol* 1993; 170: 429–434.

17. Schadendorf D, Heidel J, Gawlik C, et al. Association with clinical outcome of expression of VLA-4 in primary cutaneous malignant melanoma as well as P-selectin and E-selectin on intratumoral vessels. *J Natl Cancer Inst* 1995; 87: 366–371.

18. Lyck R, Ruderisch N, Moll AG, et al. Culture-induced changes in blood-brain barrier transcriptome: implications for amino-acid transporters in vivo. *J Cereb Blood Flow Metab* 2009; 29: 1491–1502.

19. Steiner O, Coisne C, Engelhardt B, et al. Comparison of immortalized bEnd5 and primary mouse brain microvascular endothelial cells as in vitro blood-brain barrier models for the study of T cell extravasation. *J Cereb Blood Flow Metab* 2011; 31: 315–327.

20. Moretti FA, Moser M, Lyck R, et al. Kindlin-3 regulates integrin activation and adhesion reinforcement of effector T cells. *Proc Natl Acad Sci U S A* 2013; 110: 17005–17010.

21. Rudolph H, Klopstein A, Gruber I, et al. Postarrest stalling rather than crawling favors CD8(+) over CD4(+) T-cell migration across the blood-brain barrier under flow in vitro. *Eur J Immunol* 2016; 46: 2187–2203.

22. Lyck R, Lecuyer MA, Abadier M, et al. ALCAM (CD166) is involved in extravasation of monocytes rather than T cells across the blood-brain barrier. *J Cereb Blood Flow Metab* 2017; 37: 2894–2909.

23. Reiss Y, Hoch G, Deutsch U, et al. T cell interaction with ICAM-1-deficient endothelium in vitro: essential role for ICAM-1 and ICAM-2 in transendothelial migration of T cells. *Eur J Immunol* 1998; 28: 3086–3099.

24. Laschinger M and Engelhardt B. Interaction of alpha4-integrin with VCAM-1 is involved in adhesion of encephalitogenic T cell blasts to brain endothelium but not in their transendothelial migration in vitro. *J Neuroimmunol* 2000; 102: 32–43.

25. Pulido R, Campanero MR, Garcia-Pardo A, et al. Structure-function analysis of the human integrin VLA-4 (alpha 4/beta 1). Correlation of proteolytic alpha 4 peptides with alpha 4 epitopes and sites of ligand interaction. *FEBS Lett* 1991; 294: 121–124.

26. Riedl J, Flynn KC, Raducanu A, et al. Lifeact mice for studying F-actin dynamics. *Nat Meth* 2010; 7: 168–169.

27. Rohnelt RK, Hoch G, Reiss Y, et al. Immunosurveillance modelled in vitro: naive and memory T cells spontaneously migrate across unstimulated microvascular endothelium. *Int Immunol* 1997; 9: 435–450.

28. Raaijmakers MI, Widmer DS, Maudrich M, et al. A new live-cell biobank workflow efficiently recovers heterogeneous melanoma cells from native biopsies. *Exp Dermatol* 2015; 24: 377–380.

29. Broz ML, Binnewies M, Boldajipour B, et al. Dissecting the tumor myeloid compartment reveals rare activating antigen-presenting cells critical for T cell immunity. *Cancer Cell* 2014; 26: 638–652.

30. Graf LH Jr, Kaplan P and Silagi S. Efficient DNA-mediated transfer of selectable genes and unselected sequences into differentiated and undifferentiated mouse melanoma clones. *Somat Cell Mol Genet* 1984; 10: 139–151.

31. Fan D, Liaw A, Denkins YM, et al. Type-1 transforming growth factor-beta differentially modulates tumoricidal activity of murine peritoneal macrophages against metastatic variants of the B16 murine melanoma. *J Exp Ther Oncol* 2002; 2: 286–297.

32. Coisne C, Lyck R and Engelhardt B. Live cell imaging techniques to study T cell trafficking across the blood-brain barrier in vitro and in vivo. *Fluids Barriers CNS* 2013; 10: 7.

33. Zlobec I, Suter G, Perren A, et al. A next-generation tissue microarray (ngTMA) protocol for biomarker studies. *J Vis Exp* 2014; 51893.

34. Brachtl G, Sahakyan K, Denk U, et al. Differential bone marrow homing capacity of VLA-4 and CD38 high expressing chronic lymphocytic leukemia cells. *PLoS One* 2011; 6: e23758.

35. Moore TL, Hauser D, Gruber T, et al. Cellular shuttles: monocytes/macrophages exhibit transendothelial transport of nanoparticles under physiological flow. *ACS Appl Mater Interf* 2017; 9: 18501–18511.

36. Gorina R, Lyck R, Vestweber D, et al. beta2 integrin-mediated crawling on endothelial ICAM-1 and ICAM-2 is a prerequisite for transcellular neutrophil diapedesis across the inflamed blood-brain barrier. *J Immunol* 2014; 192: 324–337.

37. Lyck R and Engelhardt B. Going against the tide – how encephalitogenic T cells breach the blood-brain barrier. *J Vasc Res* 2012; 49: 497–509.

38. Moretti FA, Moser M, Lyck R, et al. Kindlin-3 regulates integrin activation and adhesion reinforcement of effector T cells. *Proc Natl Acad Sci U S A* 2013; 110: 17005–17010.

39. Coisne C, Mao W and Engelhardt B. Cutting edge: natalizumab blocks adhesion but not initial contact of human T cells to the blood-brain barrier in vivo in an animal model of multiple sclerosis. *J Immunol* 2009; 182: 5909–5913.

40. Renz ME, Chiu HH, Jones S, et al. Structural requirements for adhesion of soluble recombinant murine vascular cell adhesion molecule-1 to alpha 4 beta 1. *J Cell Biol* 1994; 125: 1395–1406.

41. Abadier M, Jahromi NH, Alves LC, et al. Cell surface levels of endothelial ICAM-1 influence the transcellular

or paracellular T-cell diapedesis across the blood-brain barrier. *Eur J Immunol* 2015; 45: 1043–1058.

42. Taichman DB, Cybulsky MI, Djaffar I, et al. Tumor cell surface alpha 4 beta 1 integrin mediates adhesion to vascular endothelium: demonstration of an interaction with the N-terminal domains of INCAM-110/VCAM-1. *Cell Regul* 1991; 2: 347–355.

43. Martin-Padura I, Mortarini R, Lauri D, et al. Heterogeneity in human melanoma cell adhesion to cytokine activated endothelial cells correlates with VLA-4 expression. *Cancer Res* 1991; 51: 2239–2241.

44. Martinelli R, Kamei M, Sage PT, et al. Release of cellular tension signals self-restorative ventral lamellipodia to heal barrier micro-wounds. *J Cell Biol* 2013; 201: 449–465.

45. Garofalo A, Chirivi RG, Foglieni C, et al. Involvement of the very late antigen 4 integrin on melanoma in interleukin 1-augmented experimental metastases. *Cancer Res* 1995; 55: 414–419.

46. Okahara H, Yagita H, Miyake K, et al. Involvement of very late activation antigen-4 (vla-4) and vascular cell adhesion molecule-1 (vcam-1) in tumor-necrosis-factor-alpha enhancement of experimental metastasis. *Cancer Res* 1994; 54(N12): 3233–3236.

47. Qian F, Vaux DL and Weissman IL. Expression of the integrin alpha 4 beta 1 on melanoma cells can inhibit the invasive stage of metastasis formation. *Cell* 1994; 77: 335–347.

48. Brandsma D, Reijneveld JC, Taphoorn MJ, et al. Vascular cell adhesion molecule-1 is a key adhesion molecule in melanoma cell adhesion to the leptomeninges. *Lab Invest* 2002; 82: 1493–1502.

49. Gehlsen KR, Davis GE and Sriramarao P. Integrin expression in human melanoma cells with differing invasive and metastatic properties. *Clin Exp Metast* 1992; 10: 111–120.

50. Albelda SM, Mette SA, Elder DE, et al. Integrin distribution in malignant melanoma: association of the beta 3 subunit with tumor progression. *Cancer Res* 1990; 50: 6757–6764.

51. Derfuss T, Kuhle J, Lindberg R, et al. Natalizumab therapy for multiple sclerosis. *Semin Neurol* 2013; 33: 26–36.

52. Nali LH, Moraes L, Fink MC, et al. Natalizumab treatment for multiple sclerosis: updates and considerations for safer treatment in JCV positive patients. *Arq Neuropsiquiatr* 2014; 72: 960–965.

53. Zwingenberger AL, Kent MS, Shi C, et al. Affinity of the alpha4-beta1 integrin-targeting peptide LLP2A to canine lymphoma. *Vet Immunol Immunopathol* 2012; 145: 298–304.

54. Beaino W and Anderson CJ. PET imaging of very late antigen-4 in melanoma: comparison of 68Ga- and 64Cu-labeled NODAGA and CB-TE1A1P-LLP2A conjugates. *J Nucl Med* 2014; 55: 1856–1863.

55. Beaino W, Guo Y, Chang AJ, et al. Roles of Atox1 and p53 in the trafficking of copper-64 to tumor cell nuclei: implications for cancer therapy. *J Biol Inorg Chem* 2014; 19: 427–438.